Catalysis Today 180 (2012) 148–154

Contents lists available at ScienceDirect

Catalysis Today

journal homepage: www.elsevier.com/locate/cattod

Total oxidation of ethyl acetate, ethanol and toluene catalyzed by exotemplated manganese and cerium oxides loaded with gold

S.S.T. Bastos[a], S.A.C. Carabineiro[a], J.J.M. Órfão[a], M.F.R. Pereira[a], J.J. Delgado[b], J.L. Figueiredo[a,*]

[a] Laboratório de Catálise e Materiais (LCM), Laboratório Associado LSRE/LCM, Departamento de Engenharia Química, Faculdade de Engenharia, Universidade do Porto, Rua Dr. Roberto Frias, 4200-465 Porto, Portugal

[b] Departamento de Ciencia de los Materiales e Ingeniería Metalúrgica y Química Inorgánica, Facultad de Ciencias, Universidad de Cádiz, Campus Rio San Pedro, 11510 Puerto Real, Cádiz, Spain

ARTICLE INFO

Article history:
Received 10 December 2010
Received in revised form 28 January 2011
Accepted 31 January 2011
Available online 2 March 2011

Keywords:
Volatile organic compounds
Ethyl acetate
Ethanol
Toluene
Cerium oxides
Manganese oxides
Gold
Catalytic oxidation

ABSTRACT

The catalytic performance of manganese and cerium oxides synthesized by an exotemplating method was evaluated in the total oxidation of ethyl acetate, ethanol and toluene. The addition of gold to cerium and manganese oxides improved their catalytic activity in most cases, especially in the case of ceria materials. The best catalysts were able to totally convert ethanol, ethyl acetate and toluene to 100% of CO_2 at 230 °C, 250 °C and 300 °C, respectively, using a space velocity of 53,050 h^{-1} and a feed VOC concentration of 1000 mg C m^{-3} (10 mg C min^{-1} g_{cat}^{-1}). Both the pure oxides and gold catalysts were found to be stable.

1. Introduction

Volatile organic compounds (VOCs) are a major contributor to air pollution because of their toxic and malodorous nature and their involvement in ozone depletion and smog formation [1,2]. They are emitted from a wide range of industrial processes and transportation activities.

Catalytic combustion is the most promising technology for the destruction of VOCs [1,2]. This approach is preferred to the thermal one due to the lower temperature required and its greater selectivity, which implies a considerable saving of energy. Thermal oxidation needs to operate in a range of temperatures between 700 and 1000 °C, which leads to NO_x production from the N_2 present in air. In the case of catalytic oxidation, the operation temperature decreases to around 250–500 °C, therefore, NO_x production is much lower, as well as the energy needed to preheat the stream [2].

Metal oxides or supported noble metals can be used in catalytic oxidation of VOCs, manganese materials being very interesting in this context [3–11]. On the other hand, gold supported on ceria has been reported as a good catalyst for benzene, toluene, propanol, propene and formaldehyde oxidation [1,12–15].

Recently, templating methods for the preparation of porous metal oxides have been reported [8,16–24]. Templating synthesis can be distinguished according to the way the template acts [18]. Templates that are occluded in the growing solid and leave a pore system after their removal are called “endotemplates”. Alternatively, if the template is a material with structural pores in which another solid is created, thus providing a scaffold for the synthesis, it is called an “exotemplate”. In both procedures, the template is removed in order to obtain high-surface area pure materials [18].

Carbon templates are attractive due to their high-surface area and porosity, low cost and because they are easily removed by combustion. This approach has been successfully used for the synthesis of high-surface area metal and mixed metal oxides like Al_2O_3, CeO_2, Cr_2O_3, Fe_2O_3, MgO, MnO_x,TiO_2 using activated carbons [16–18,21], activated carbon fibers [18,21], carbon nanotubes [25] and carbon aerogels [20] as templates.

In previous papers, our group reported on the synthesis of manganese [8,24] and cerium [23] oxides by exotemplating, using activated carbons and carbon xerogels, with different textural

* Corresponding author. Tel.: +351 22 508 1663; fax: +351 22 508 1449.
E-mail addresses: sandra.bastos@fe.up.pt (S.S.T. Bastos), sonia.carabineiro@fe.up.pt (S.A.C. Carabineiro), jjmo@fe.up.pt (J.J.M. Órfão), fpereira@fe.up.pt (M.F.R. Pereira), juanjose.delgado@uca.es (J.J. Delgado), jlfig@fe.up.pt (J.L. Figueiredo).

0920-5861/$ – see front matter © 2011 Elsevier B.V. All rights reserved.
doi:10.1016/j.cattod.2011.01.049

properties and surface chemistries, as templates. The resulting exotemplated materials were loaded with gold and tested for the oxidation of CO, which is an important reaction in pollution control (CO removal), fuel-cells, and gas sensing [1,26]. Moreover, the study of CO oxidation is also important in this context, CO being a possible by-product in VOC oxidation (since the complete oxidation of the pollutant to CO_2 does not always take place [27]).

In the present work, selected exotemplated manganese and cerium oxide catalysts, pure or loaded with gold, which were already used in the oxidation of CO in previous works [23,24], were tested in the oxidation of VOCs, namely ethyl acetate, ethanol and toluene.

2. Experimental

2.1. Synthesis

Manganese and cerium oxides were synthesized by exotemplating with carbon materials, following the procedures described in earlier papers [8,23,24]. Two different techniques were used for exotemplate synthesis: incipient wetness (IW) and excess solution impregnation (EI). Other Mn and Ce oxides were synthesized by traditional methods (direct calcination of the precursor or its precipitation with sodium hydroxide) in order to compare their catalytic performances with those prepared by exotemplating. A summary of the samples used in this work is shown in Table 1. Further details can be found elsewhere [8,23,24].

Au was loaded on the supports by the double impregnation method (DIM) using $HAuCl_4{\cdot}3H_2O$ as the gold precursor (Alfa Aesar) in order to achieve 1 wt.% nominal content of Au, as described earlier [23,24]. The materials prepared were used with no further treatment.

2.2. Characterization

Manganese and cerium oxides were characterized by adsorption of N_2 at −196 °C and temperature programmed reduction (TPR), under H_2 atmosphere, as described in previous works [23,24]. Selected samples were characterized by field emission scanning electron microscopy/energy dispersive X-ray spectroscopy (FESEM–EDS), X-ray diffraction (XRD), X-ray photoelectron spectroscopy (XPS), high resolution transmission electron microscopy (HRTEM), high-angle annular dark-field imaging (HAADF) and inductively coupled plasma/atomic emission spectroscopy (ICP–AES). Further details can be found elsewhere [8,23,24].

2.3. Catalytic experiments

The catalyst samples (50 mg) were pretreated under air flow for 1 h before reaction. This pretreatment was conducted at room temperature for supported gold catalysts, while the supports were heated up to 400 °C. The catalytic oxidation of ethyl acetate, ethanol and toluene was performed under atmospheric pressure using a VOC composition of 1000 mg C m^{-3} (~466 ppmv of ethyl acetate, ~930 ppmv of ethanol and ~266 ppmv of toluene) or 10 mg C min^{-1} g_{cat}^{-1}. The feed stream of 500 cm^3 min^{-1} (PTN), which corresponds to a space velocity of 53,050 h^{-1} (determined in terms of total bed volume), was heated at a rate of 2.5 °C min^{-1}. A fixed-bed reactor was placed inside a temperature controlled electrical furnace and the temperature in the reaction zone was measured by a K type thermocouple placed in the middle of the catalyst bed. In order to minimize thermal effects, the catalyst was mixed with an inert (Carborundum, CSi, from VWR). The outgoing stream from the reactor was analyzed by a CO_2 non-dispersive infrared (NDIR) sensor Vaisala GMT220, a CO ToxiPro (Biosystems) sensor and a total volatile organic compounds analyzer MiniRAE2000.

The reaction was carried out in two cycles of increasing and decreasing temperature. The conversion into CO_2 (X_{CO_2}) was calculated as $X_{CO_2} = F_{CO_2}/(\nu_{voc}\, F_{VOC,in})$ where $F_{VOC,in}$ is the inlet molar flow rate of VOC, F_{CO_2} is the outlet molar flow rate of CO_2 and ν_{voc} is the number of carbon atoms in the VOC molecule ($\nu_{ethyl\ acetate} = 4$, $\nu_{ethanol} = 2$ and $\nu_{toluene} = 7$).

3. Results and discussion

3.1. Characterization

Table 1 shows the characterization results for the oxide samples. The surface area of the ceria exotemplated materials is similar to that of samples prepared by standard calcination and precipitation methods, unlike the results obtained with manganese oxides, which increased up to seven fold.

FESEM showed that all the ceria materials look very similar, as can be seen in Fig. 1a–d, having a "cottonlike" appearance. Mn1 sample (Fig. 1e) has a homogeneous surface with prismatic shaped particles of 30–50 nm length. Mn2 (Fig. 1f) has a very heterogeneous surface, showing prismatic shaped particles with very different sizes. The microstructure of Mn10 consists of quadrangular prisms (not shown), which are similar to those observed with Mn1. As reported in previous papers [8,24] these observations are related to the different phases formed, which are displayed in Table 1. The average oxidation state of Mn in these materials was between 2.45 and 3.30 (as determined by XPS), which is in agreement with the mixture of manganese phases in each sample [8,24]. Ceria materials showed the same phase (cerianite CeO_2), as detected by XRD. XPS results were very similar and allowed to determine the percentage of Ce (IV) on the surface, which varied from 76 to 83% [23].

Selected samples were analyzed by HRTEM and HAADF. Fig. 2a shows one image of the Ce8 support. Its appearance is of ultrafine

Table 1
Characterization of oxides and supported gold catalysts.

Oxide supports						Au/oxide supports		
Sample	Template	Method	BET (m^2/g)[a]	Phases detected by XRD[a]	First peak of TPR (°C)[a]	First peak of TPR (°C)[a]	Au particle size (nm)	Au loading (%)
Ce1	–	Precipitation with NaOH	150	CeO_2	430	125	n.d.	0.77
Ce2	–	Calcination of the precursor	98	n.d.	420	175	6–12[a]	0.84
Ce7	Carbon xerogel	Exotemplating by EI	96	n.d.	250	105	n.d.	n.d.
Ce8	Carbon xerogel	Exotemplating by IW	96	CeO_2	280	105	5–10[a]	0.75[a]
Mn1	–	Precipitation with NaOH	31	Mn_5O_8	240	250	[b]	0.97
Mn2	–	Calcination of the precursor	18	Mn_3O_4 (60%); Mn_2O_3 (40%)	230	430	[b]	1.08
Mn4	Activated carbon	Exotemplating by EI	84	n.d.	290	220	4–11	0.78
Mn10	Carbon xerogel	Exotemplating by EI	124	Mn_3O_4 (92%); Mn_2O_3 (8%)	265	266	[b]	0.86

[a] From Refs. [8,23,24].
[b] Only large crystals (>15 nm) were detected.

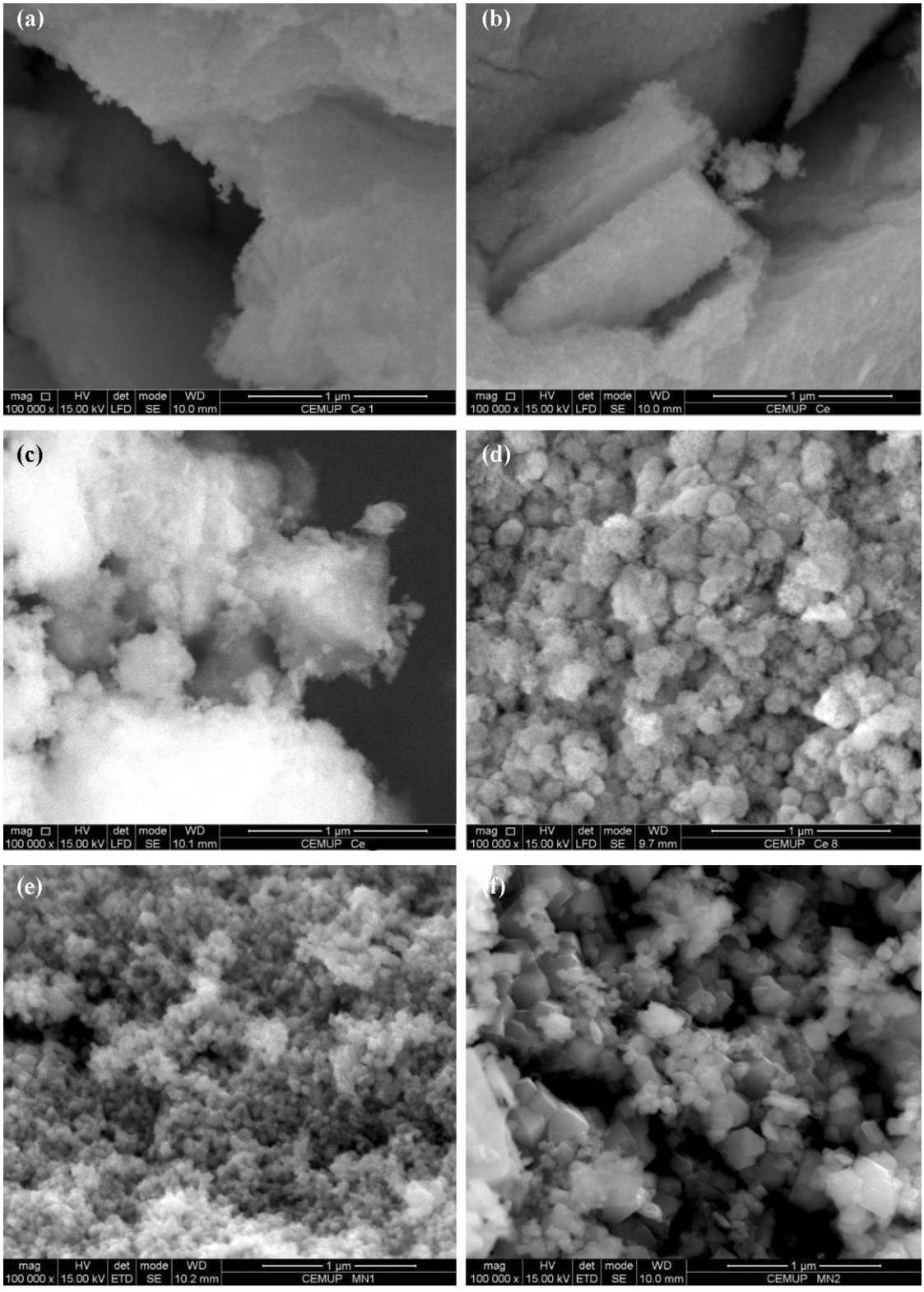

Fig. 1. FESEM images of samples Ce1 (a), Ce2 (b), Ce7 (c), Ce8 (d), Mn1 (e) and Mn2 (f).

agglomerated crystallites, in different forms, with a body diagonal of ~3–6 nm. These nanoparticles of ceria have different orientations and in some cases rounded edges are observed, as seen with solvothermal ceria [28,29].

Fig. 2b shows a HRTEM image of a gold nanoparticle on the Ce8 support while Fig. 2c shows an HAADF image of a gold nanoparticle on the Mn4 support. The low metal loading and the high-surface area of the catalysts prevented to obtain the particle size distributions, since not many particles were visible, as found in earlier works [23]. However, estimations of the gold nanoparticle sizes are displayed in Table 1. The particle size range observed for the gold supported catalyst was between 5 and 12 nm for the Au/ceria materials [23]. The size of gold nanoparticles detected was larger in the manganese oxide materials, as expected from an earlier work [24],

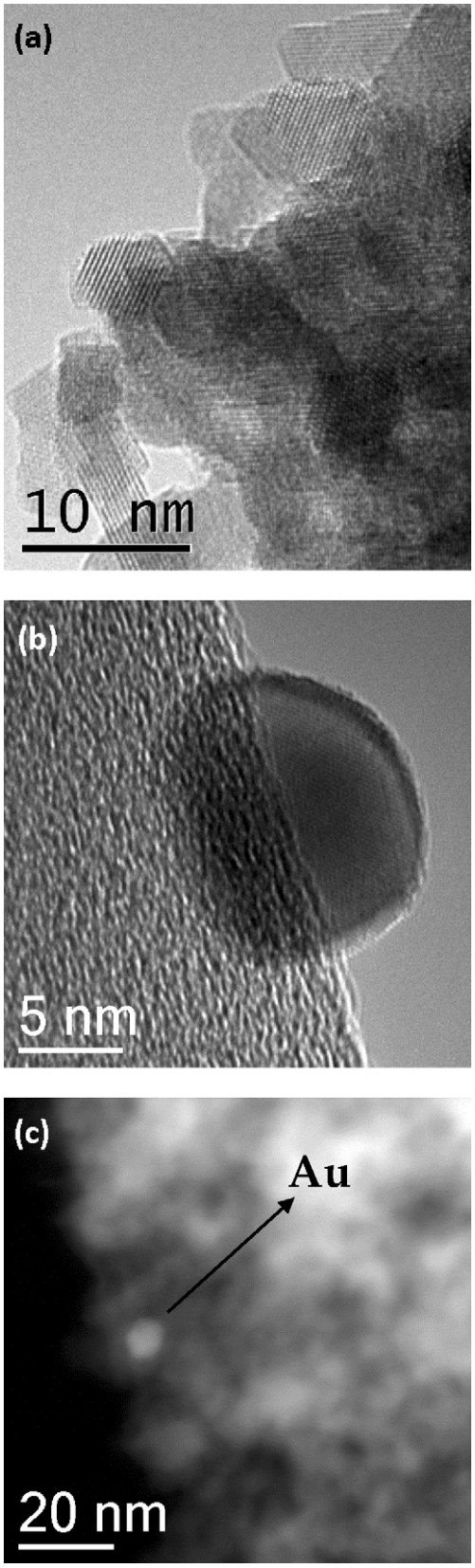

Fig. 2. HRTEM images of the Ce8 support (a) and of a gold particle on Au/Ce8 (b). HAADF image of a gold particle on Au/Mn4 (c).

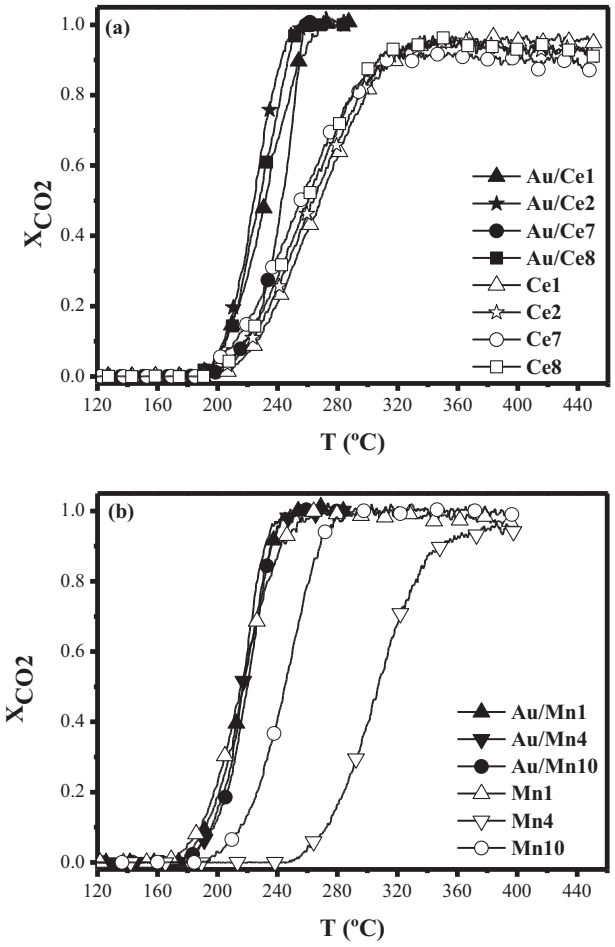

Fig. 3. Performance of the cerium and manganese oxide catalysts in the oxidation of ethyl acetate (space velocity = 53,050 h^{-1}, $C_{VOC,in}$ = 1000 mg C m^{-3}): (a) Au/CeO_2 versus CeO_2; (b) Au/MnO_x versus MnO_x. The curves are continuous, symbols are added only for identification.

being above 15 nm for all samples, except for Mn4 (for which the size varied from 4 to 11 nm).

ICP–AES results allowed to determine the gold loading (Table 1). A range between 0.75% and 0.84% was obtained for Au/Ce samples, while the gold loading for Au/Mn samples varied from 0.78% to 1.08%.

H_2-TPR experiments were carried out both for the oxides alone and loaded with gold. Not much difference was observed with the manganese oxide materials, as referred in a previous work [24], i.e., the same peaks were observed corresponding to the progressive reduction of the manganese oxides, which agree well with the results obtained by XRD. Concerning the ceria materials, loading gold onto the supports shifted the peak corresponding to the reduction of surface oxygen to much lower temperatures (~100–200 °C), while the bulk oxygen peak (~800 °C) was not significantly affected [23]. The temperature values for the first peak obtained in the TPR spectra for the oxide catalysts, with or without gold, are shown in Table 1.

3.2. Catalytic experiments

3.2.1. Screening tests

The catalytic activities for the total oxidation of ethyl acetate (Fig. 3), ethanol (Fig. 4) and toluene (Fig. 5) for the cerium and manganese oxides, alone and loaded with gold, were evaluated in order to determine the effect of the physical and chemical properties of the materials. Light-off curves of a standard experiment

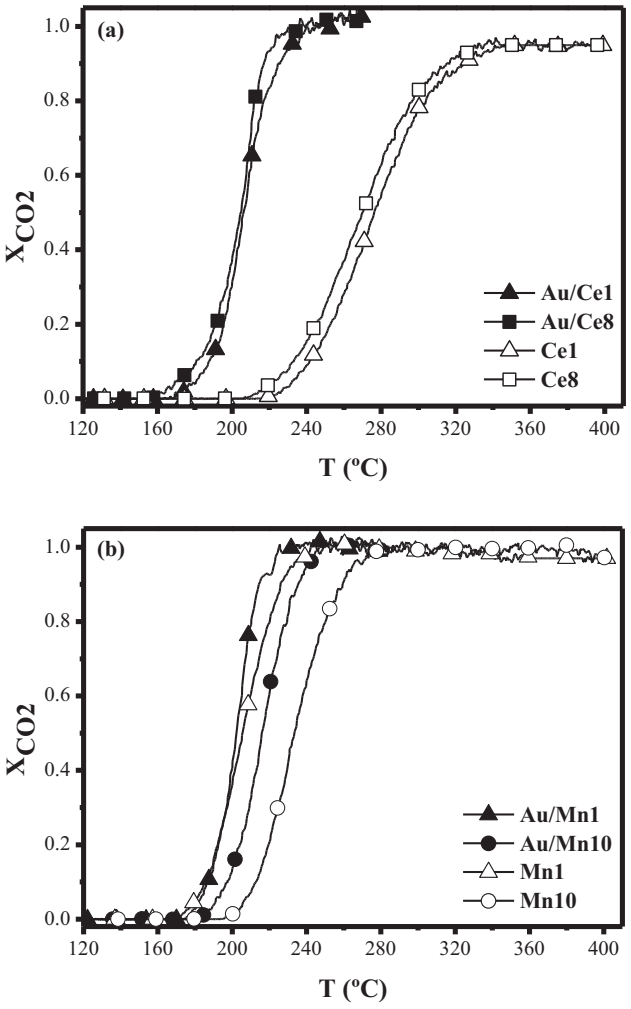

Fig. 4. Performance of the cerium and manganese oxide catalysts in the oxidation of ethanol (space velocity = 53,050 h^{-1}, $C_{VOC,in}$ = 1000 mg C m^{-3}): (a) Au/CeO_2 versus CeO_2; (b) Au/MnO_x versus MnO_x. The curves are continuous, symbols are added only for identification.

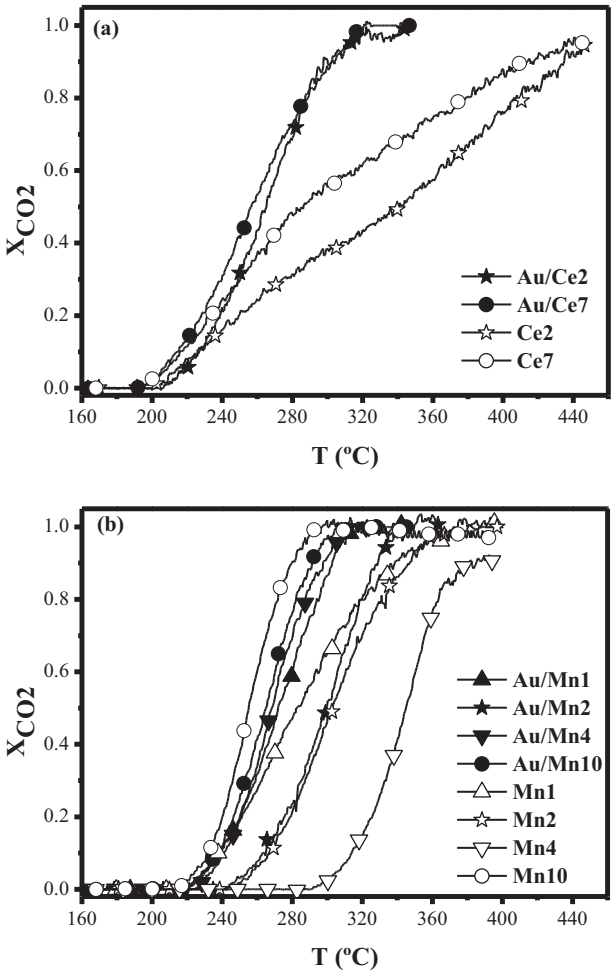

Fig. 5. Performance of the cerium and manganese oxide catalysts in the oxidation of toluene (space velocity = 53,050 h^{-1}, $C_{VOC,in}$ = 1000 mg C m^{-3}): (a) Au/CeO_2 versus CeO_2; (b) Au/MnO_x versus MnO_x. The curves are continuous, symbols are added only for identification.

consist in two cycles of: increasing temperature, keeping the temperature constant for 1 h and decreasing it, as shown in a previous work [8]. The catalytic performance in the increasing temperature step in both cycles was found to be quite similar, and the same is true for the decreasing temperature step. This is a clear indication of the stability of these catalysts.

As can be seen in Fig. 3a, the addition of gold to cerium oxides improves their catalytic performances. In fact, the support itself is not able to completely oxidize ethyl acetate up to 450 °C, CO being detected as a by-product. Total conversion of ethyl acetate with gold supported on cerium oxides is achieved at ~260 °C. This is most likely due to the remarkable capacity of these Au/ceria materials to oxidise CO, as shown in a previous paper [23]. The activity of Au/CeO_2 catalyst has been explained by the ability of gold nanoparticles to increase the mobility of lattice oxygen by weakening the Ce–O bonds adjacent to Au atoms, which increases the lattice oxygen donating ability of CeO_2 to oxidize the VOC molecule through a Mars-van Krevelen reaction mechanism [13]. In fact, a correlation was found between the catalytic activity of ceria samples and the temperature of the first peak of the TPR spectra, that is related with the oxygen reactivity of these samples. Apparently, the cerium oxides synthesis is not much relevant for Au/Ce catalytic performance because their light-off curves are similar, with the exception of Au/Ce7 that has a slightly worse performance between 200 and ~240 °C. Our results for ethyl acetate oxidation on Au/Ce catalysts are in agreement with other ceria supported noble metal catalysts, such as Pt/CeO_2, Pd/CeO_2, Ru/CeO_2 and Rh/CeO_2, which can oxidize this type of VOC molecule into 100% of CO_2 up to 250 °C [30], but using a space velocity of 15,000 h^{-1} while we used 53,050 h^{-1}.

There are a few differences in the total oxidation of ethyl acetate on gold supported manganese oxides, as showed in Fig. 3b. For sample Mn1, which was found to be one of the best catalysts in our previous work on ethanol oxidation [8], the addition of gold does not improve its catalytic performance. This is most likely due to the large particle size of gold particles found in this catalyst (>15 nm), well known to be inversely related with catalytic activity [1,26]. However, in the case of the samples Mn4 (prepared with activated carbon as template) and Mn10 (prepared with carbon xerogel as template), adding gold to these manganese oxides increases their catalytic activities, the effect being more considerable in the case of Mn4, which is not able to oxidize ethyl acetate to 100% of CO_2 up to 400 °C by itself, leading to the formation of some CO as a by-product. When gold is added to Mn4, total conversion of ethyl acetate to CO_2 is possible at ~250 °C. This could be explainable with the smaller particle size of gold particles (4–11 nm) found in this catalyst (Table 1).

Catalytic results for the total oxidation of ethanol are shown in Fig. 4. Similar trends to those obtained in the ethyl acetate oxidation experiments were observed. It was shown in a previous paper [8] that the lattice oxygen of the manganese oxide can react

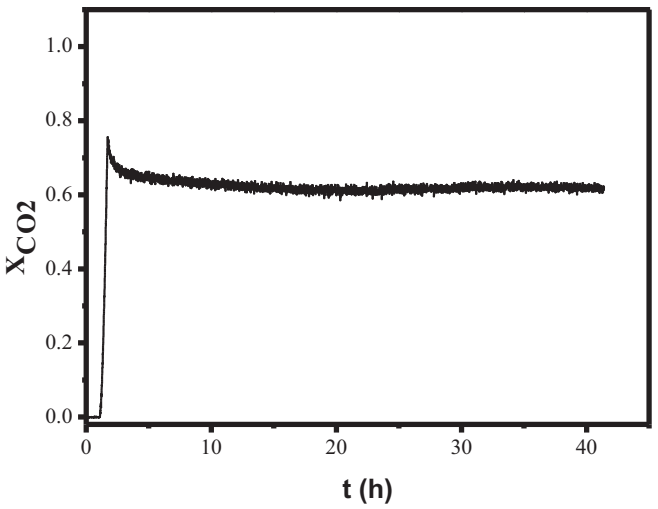

Fig. 6. Influence of time on stream in the oxidation of ethyl acetate (space velocity = 53,050 h^{-1}, $C_{VOC,in}$ = 1000 mg C m^{-3}) at 260 °C over Ce7.

with ethanol and is involved in the ethanol oxidation mechanism, a strong correlation between catalytic activity and the lattice oxygen donating ability being found. Therefore, as in the case of ethyl acetate, the reactivity follows the order of the TPR peaks. It is interesting to notice that addition of gold has a larger effect on the ceria materials (Fig. 4a) than on the manganese oxides (Fig. 4b). This is most likely due to fact that the particle size of gold is lower on cerium than on manganese oxides (as seen in Table 1).

Selected samples were also tested in the total oxidation of toluene, and these results are shown in Fig. 5. Addition of gold to ceria causes total oxidation to occur at ~320 °C, while the supports alone are not able to achieve it. Again, this might be related with the high activity of ceria materials loaded with gold to oxidise CO [23], which is a by-product of the oxidation of VOCs.

Sample Mn10 was found to be the best catalyst for the total oxidation of toluene, possibly because it has the largest surface area (Table 1). Addition of gold to this sample does not improve its catalytic activity, possibly as a result of the large particle size detected. In the case of Mn1 and Mn2, addition of gold improves the conversion into CO_2, possibly as a result of the gold activity found for CO oxidation [24], which was the main by-product detected during toluene oxidation in the presence of manganese oxides. On the other hand, the significant enhancement in the activity of Mn4 after gold loading may be related to the smaller gold particle size of sample Au/Mn4.

3.2.2. Stability tests

In order to evaluate the stability of the gold catalysts presented in this work for the total oxidation of VOC, long term experiments were performed for ethyl acetate oxidation. Fig. 6 shows the influence of time on stream in the oxidation of ethyl acetate at 260 °C over Ce7. It can be seen that the catalyst is stable for at least 40 h. Similar results were obtained with other samples, with or without gold.

4. Conclusions

Manganese and cerium oxides were synthesized by exotemplating using activated carbon and carbon xerogel as templates. Au was loaded into these materials by a double impregnation method. The oxides alone and the oxides loaded with gold, were tested in the total oxidation of ethyl acetate, ethanol and toluene. The addition of gold to cerium oxides improved significantly their catalytic activity. In the case of manganese oxides, the addition of gold did not always produce better results (as for Mn1 and Mn10 samples in the oxidation of ethyl acetate and toluene, respectively, where results with and without gold are similar). However, the addition of gold improved the activity of the manganese oxide catalysts that were less active (namely the Mn4 sample). The best Au/CeO_2 and Au/MnO_x catalysts were able to oxidize ethyl acetate into 100% of CO_2 at ~250 °C. Total oxidation of ethanol was achieved at 230 °C using Au/Mn1 as catalyst. Toluene was the most difficult VOC molecule to oxidize, and this was only accomplished at 300 °C with the Mn10 catalyst. Both CeO_2 and MnO_x catalysts, with or without gold, were found to be stable during VOC oxidation.

Acknowledgements

This work was supported by Fundação para a Ciência e a Tecnologia (FCT) and FEDER, under Programs POCI 2010 and COMPETE, Project PTDC/AMB/69065/2006. S.A.C. is grateful to FCT for financing (CIENCIA 2007 program).

References

[1] S.A.C. Carabineiro, D.T. Thompson, Catalytic applications for gold nanotechnology, in: U. Heiz, U. Landman (Eds.), Nanocatalysis, Springer-Verlag, Berlin, Heidelberg, New York, 2007, pp. 377–489.
[2] T. Garetto, Í. Legorburu, M. Montes, Eliminación de emisiones atmosféricas de COVs por catálisis y adsorción, Programa CYTED, Argentina, 2008.
[3] C. Lahousse, A. Bernier, P. Grange, B. Delmon, P. Papaefthimiou, T. Ioannides, X. Verykios, Evaluation of γ-MnO_2 as a VOC removal catalyst: comparison with a noble metal catalyst, J. Catal. 178 (1998) 214–225.
[4] K.M. Parida, A. Samal, Catalytic combustion of volatile organic compounds on Indian Ocean manganese nodules, Appl. Catal. A-Gen. 182 (1999) 249–256.
[5] J. Luo, Q. Zhang, A. Huang, S.L. Suib, Total oxidation of volatile organic compounds with hydrophobic cryptomelane-type octahedral molecular sieves, Micropor. Mesopor. Mater. 35–36 (2000) 209–217.
[6] E. Finocchio, G. Busca, Characterization and hydrocarbon oxidation activity of coprecipitated mixed oxides Mn_3O_4/Al_2O_3, Catal. Today 70 (2001) 213–225.
[7] F. Aguero, A. Scian, B. Barbero, L. Cadús, Influence of the support treatment on the behavior of MnO_x/Al_2O_3 catalysts used in VOC combustion, Catal. Lett. 128 (2009) 268–280.
[8] S.S.T. Bastos, J.J.M. Órfão, M.M.A. Freitas, M.F.R. Pereira, J.L. Figueiredo, Manganese oxide catalysts synthesized by exotemplating for the total oxidation of ethanol, Appl. Catal. B-Environ. 93 (2009) 30–37.
[9] V.P. Santos, M.F.R. Pereira, J.J.M. Órfão, J.L. Figueiredo, Catalytic oxidation of ethyl acetate over a cesium modified cryptomelane catalyst, Appl. Catal. B-Environ. 88 (2009) 550–556.
[10] V.P. Santos, M.F.R. Pereira, J.J.M. Órfão, J.L. Figueiredo, Synthesis and characterization of manganese oxide catalysts for the total oxidation of ethyl acetate, Top. Catal. 52 (2009) 470–480.
[11] V.P. Santos, M.F.R. Pereira, J.J.M. Órfão, J.L. Figueiredo, The role of lattice oxygen on the activity of manganese oxides towards the oxidation of volatile organic compounds, Appl. Catal. B-Environ. 99 (2010) 353–363.
[12] F. Pinna, Supported metal catalysts preparation, Catal. Today 41 (1998) 129–137.
[13] S. Scirè, S. Minicò, C. Crisafulli, C. Satriano, A. Pistone, Catalytic combustion of volatile organic compounds on gold/cerium oxide catalysts, Appl. Catal. B-Environ. 40 (2003) 43–49.
[14] Y. Shen, X. Yang, Y. Wang, Y. Zhang, H. Zhu, L. Gao, M. Jia, The states of gold species in CeO_2 supported gold catalyst for formaldehyde oxidation, Appl. Catal. B-Environ. 79 (2008) 142–148.
[15] P. Lakshmanan, L. Delannoy, V. Richard, C. Méthivier, C. Potvin, C. Louis, Total oxidation of propene over $Au/xCeO_2–Al_2O_3$ catalysts: Influence of the CeO_2 loading and the activation treatment, Appl. Catal. B-Environ. 96 (2010) 117–125.
[16] H. Wakayama, H. Itahara, N. Tatsuda, S. Inagaki, Y. Fukushima, Nanoporous metal oxides synthesized by the nanoscale casting process using supercritical fluids, Chem. Mater. 13 (2001) 2392–2396.
[17] M. Schwickardi, T. Johann, W. Schmidt, F. Schüth, High-surface-area oxides obtained by an activated carbon route, Chem. Mater. 14 (2002) 3913–3919.
[18] F. Schüth, Endo- and exo-templating to create high-surface-area inorganic materials, Angew. Chem. Int. Ed. 42 (2003) 3604–3622.
[19] S.C. Laha, R. Ryoo, Synthesis of thermally stable mesoporous cerium oxide with nanocrystalline frameworks using mesoporous silica templates, Chem. Commun. (2003) 2138–2139.
[20] W.C. Li, A.H. Lu, C. Weidenthaler, F. Schüth, Hard-templating pathway to create mesoporous magnesium oxide, Chem. Mater. 16 (2004) 5676–5681.
[21] M. Crocker, G. Jacobs, A.M. Rubel, R. Andrews, U.M. Graham, E. Morris, R. Gonzalez, Preparation and characterization of cerium oxide templated from activated carbon, J. Mater. Sci. 42 (2007) 3454–3464.
[22] Y. Ren, Z. Ma, L. Qian, S. Dai, H. He, P. Bruce, Ordered crystalline mesoporous oxides as catalysts for CO oxidation, Catal. Lett. 131 (2009) 146–154.

[23] S.A.C. Carabineiro, S.S.T. Bastos, J.J.M. Órfão, M.F.R. Pereira, J.J. Delgado, J.L. Figueiredo, Exotemplated ceria catalysts with gold for CO oxidation, Appl. Catal. A-Gen. 381 (2010) 150–160.
[24] S.A.C. Carabineiro, S.S.T. Bastos, J.J.M. Órfão, M.F.R. Pereira, J.J. Delgado, J.L. Figueiredo, Carbon monoxide oxidation catalysed by exotemplated manganese oxides, Catal. Lett. 134 (2010) 217–227.
[25] D. Zhang, C. Pan, L. Shi, L. Huang, J. Fang, H. Fu, A highly reactive catalyst for CO oxidation: CeO_2 nanotubes synthesized using carbon nanotubes as removable templates, Micropor. Mesopor. Mater. 117 (2009) 193–200.
[26] S.A.C. Carabineiro, D.T. Thompson, Gold catalysis, in: C. Corti, R. Holliday (Eds.), Gold: Science and Applications, CRC Press, Taylor and Francis Group, Boca Raton, London, New York, 2010, pp. 89–122.
[27] V.P. Santos, S.A.C. Carabineiro, P.B. Tavares, M.F.R. Pereira, J.J.M. Órfão, J.L. Figueiredo, Oxidation of CO, ethanol and toluene over TiO_2 supported noble metal catalysts, Appl. Catal. B-Environ. 99 (2010) 198–205.
[28] S.A.C. Carabineiro, A.M.T. Silva, G. Dražić, P.B. Tavares, J.L. Figueiredo, Gold nanoparticles on ceria supports for the oxidation of carbon monoxide, Catal. Today 154 (2010) 21–30.
[29] S.A.C. Carabineiro, A.M.T. Silva, G. Drazic, P.B. Tavares, J.L. Figueiredo, Effect of chloride on the sinterization of Au/CeO_2 catalysts, Catal. Today 154 (2010) 293–302.
[30] T. Mitsui, T. Matsui, R. Kikuchi, K. Eguchi, Low-temperature complete oxidation of ethyl acetate over CeO_2-supported precious metal catalysts, Top. Catal. 52 (2009) 464–469.